



# Empirical Modelling and Optimization of Ngbo Pillarred Activated Clay Catalysts using Response Surface Methodology

V. N. Nwobasi <sup>a\*</sup>, Philomena K. Igbokwe <sup>b</sup> and Akindele O. Okewale <sup>c</sup>

<sup>a</sup> Department of Food Science and Tech, EBSU, Abakaliki, Nigeria.

<sup>b</sup> Department of Chemical Engineering, UNIZIK, Awka, Nigeria.

<sup>c</sup> Department of Chemical Engineering, Federal University of Petroleum Resources, Effurun, Delta State, Nigeria.

## Authors' contributions

*This work was carried out in collaboration among all authors. All authors read and approved the final manuscript.*

## Article Information

DOI: 10.9734/AJOCS/2022/v12i119137

## Open Peer Review History:

This journal follows the Advanced Open Peer Review policy. Identity of the Reviewers, Editor(s) and additional Reviewers, peer review comments, different versions of the manuscript, comments of the editors, etc are available here: <https://www.sdiarticle5.com/review-history/87836>

**Original Research Article**

**Received 26 March 2022**

**Accepted 01 June 2022**

**Published 08 July 2022**

## ABSTRACT

In this work, Box-Behnken's Response Surface Methodology (RSM) was applied to study the esterification reaction effectiveness of Ngbo pillarred activated clay catalyst. The esterification was monitored based on temperature, time duration, amount of reactant, catalyst weight, and particle size. The Box--Behnken's Response Surface Methodology indicates that the pillarred clay-catalyzed esterification reactions proceed through dual Acid-complex and Alcohol-complex mechanisms, with the Alcohol mechanism dominating. The esterification efficiencies of acetic acid and ethanol by acid-activated Ngbo clay catalyst optimized using RSM models indicated the estimated esterification percentage of >99%. The predicted and experimental values under the same conditions showed less than 5% difference, making the Box-Behnken design approach an efficient, effective, and reliable method for the esterification of acetic acid with ethanol. The produced catalyst was optimized using A-One way ANOVA modelling, which indicated the correlation coefficient of the regression of 0.8674, implying that 86.74% of the total variation in the esterification reaction was attributed to the experimental variables. The result obtained indicated that the process could be applied in the esterification of acetic acid to avoid the drawbacks of corrosion, loss of catalyst and environmental problems.

\*Corresponding author: E-mail: [nwobasiveronica@yahoo.com](mailto:nwobasiveronica@yahoo.com);

**Keywords:** Optimization; characterization; esterification; pillared activated clay catalyst; response surface methodology; box-behnken design.

## 1. INTRODUCTION

Esterification reactions have long been carried out in homogeneous phase in the presence of acid catalysts such as sulphuric acid, hydrochloric acid and p – toluene sulfonic acid (p – TSOH), which has drawbacks of corrosion, loss of catalyst and environmental problems [1,2]. Therefore, research has been focused on developing eco-friendly heterogeneous catalysts to synthesize fatty acid esters. The most popular solid acids catalyst used to produce esters were ion-exchange organic resins, such as Amberlyst – 15 [3,4], Zeolites [5–7] and Silica-supported heteropoly acid [8] and [9]. Nevertheless, they have shown limitations in the applicability for catalysing esterification reactions due to low thermal stability (Amberlyst-15 < 140°C), mass transfer resistance (Zeolites) [10,11], or loss of active acid sites in the presence of a polar medium (HPA/silica) [9].

Clay is one of the raw materials in abundance in Nigeria. It is readily available in Nigeria in large deposits, yet its potential has not been fully explored. However, there is recent interest in exploring the potential of clays, such as the bleaching of palm oil [12,13], in adsorption of dyes [14–16], among others. In a quest to develop green processes, clay is mostly used to synthesize catalysts. However, the use of Nigerian clays from Ngbo, Ohaukwu- Ebonyi State for producing clay catalysts is limited in the literature. However, the kinetics of clay-catalyzed esterification reactions is abundant in literature, but with little or no data on the mechanical and empirical modelling of the use of Ngbo clay in this regard.

Response Surface Methodology (RSM) collects statistical and mathematical techniques that uses quantitative data. Central composite design (CCD), Box-Behnken and Doehlert designs (BBD) are the principal response surface methodologies used in experimental design. This method is suitable for fitting a quadratic surface. It helps optimize the effective parameters with a minimum number of experiments and analyzes the interaction between the parameters [4]. The objective is to optimize a response (output variable) influenced by several independent variables (input variables). The application of RSM to design optimization aims to reduce the

cost of expensive numerous experiments, save time, reduce stress, etc [17–20].

This work investigated the use of local clay from Ngbo in Ohaukwu Local Government Area of Ebonyi State Nigeria for the production of pillared activated catalyst. It optimized the effectiveness of the clay catalyst for esterification of acetic acid with ethanol using Response Surface Methodology.

## 2. MATERIALS AND METHODS

### 2.1 Source of Raw Materials

The clay sample was obtained from Ngbo in Ohaukwu L.G.A. of Ebonyi State (N 06°30' 32.8", (E 007°58'13.7"). The dye was purchased from a chemical shop at Ogbete main market, Enugu, Enugu State. Other chemicals such as acetic acid, sodium hydroxide, aluminium trichloride (AlCl<sub>3</sub>), distilled water, etc were of standard grade.

### 2.2 Physico-chemical Characterization of Ngbo Clay

The Ngbo clay sample was subjected to physical analysis to obtain their physical properties. The analysis carried out includes: Bulk density, Moisture content, pH and Loss of Ignition (LOI).

### 2.3 Characterisation of the Raw Clay and Pillared Activated Sample

The Ngbo clay sample was characterized using XRF and SEM.

### 2.4 Clay Pillaring

The pillared clay was prepared according to the method described by Huan-Yan Xu *et al* (2009) with some modification. The pillaring agent used was an aluminium polioxonocation prepared by basic hydrolysis of an aluminium trichloride (AlCl<sub>3</sub>). A 0.20m/dm<sup>3</sup> of sodium hydroxide (NaOH) solution was poured at 4ml/min over the 0.2m AlCl<sub>3</sub> salt solution and stirred vigorously until a molar ratio OH/Al of 2 was reached. The final pH was 3.5 and the solution was kept for 1 hour at 50°C.

100g of clay sample were suspended in distilled water and stirred continuously for 30 min after which the pillaring agent solution was added (4ml/min) over the clay suspension while stirred vigorously. The final Aluminium/clay was 2mol/g. The resulting suspension was kept at 80°C for 4 hours. The solid was recovered by filtration and oven-dried at 450°C. The clay sample was pulverized and stored in an airtight container.

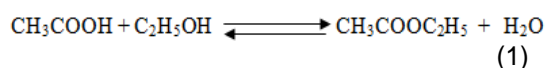
For five factors inputs of  $x_1, x_2, x_3, x_4$  and  $x_5$ , the equation of the quadratic response is given as;

$$Y = b_0 + b_1X_1 + b_2X_2 + b_3X_3 + b_4X_4 + b_5X_5 + b_{12}X_1X_2 + b_{13}X_1X_3 + b_{14}X_1X_4 + b_{15}X_1X_5 + b_{23}X_2X_3 + b_{24}X_2X_4 + b_{25}X_2X_5 + b_{34}X_3X_4 + b_{35}X_3X_5 + b_{45}X_4X_5 + b_{11}X_1^2 + b_{22}X_2^2 + b_{33}X_3^2 + b_{44}X_4^2 + b_{55}X_5^2 \quad (3)$$

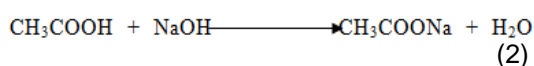
## 2.5 Optimization of Process Conditions on the Catalyst Quality Produced using Esterification Process

### 2.5.1 Sample preparation/procedure

The raw clay sample was crushed, sieved at 100microns, 200microns and 300microns. Thereafter, the clay sample was activated using pillaring agent. The activated clay sample was used in esterification reaction to assess the effectiveness. Predetermined weight of the clay sample was weighed; one mole of Ethanol and acetic acid was each pipetted into the clay sample to ensure that the active sites of the catalyst were not blocked by the ethanol. The container was tightly closed, the contents was shaken vigorously and immersed in a water bath shaker maintained at the conditions of the experimental design in Table.1. The summary of the reaction equation is:



On titration, the equation becomes:



The clay-catalysed esterification was modelled using Box-Behnken Response Surface Methodology.

## 2.6 Response Surface Methodology

The response surface technique applying Box-behnken design matrix was applied to study the interaction and effects among the factors and their level of contributions and significance in the clay-catalysed esterification. This method determines the needed best working conditions in a shorter time and detailed conditions of processes are provided. This was achieved through a designed experimental design applying Box-Behnken Response Surface Methodology design of 46 steps of experiment consisting five factors and three levels (Table 4). The numerical optimization method of RSM was used in the optimization.

## 3. RESULTS AND DISCUSSION

### 3.1 Physical Properties of the Raw Clay

The result of the physical properties of raw Ngbo clay is presented in table 3. The result showed that the clay has a moisture content of 3.3 % and bulk density of 1.25 g/ml, which are in agreement with the previous research of [22–24] that reported the moisture content of kaolinite clay is between 3.0 – 4.0% and the bulk density is 1.2 – 1.4 g/ml.

**Table 1. The natural and coded values of the independent variables used**

Variables	Natural values			Coded values		
	Low level	Mid-point	High level	Low level	Mid Point	High level
Temperature (°C), A	50	70	90	-1	0	+1
Process duration (minutes), B	30	195	360	-1	0	+1
Excess reactant (ml), C	2.5	3.75	5	-1	0	+1
Catalyst weight (grammes), D	0.25	0.38	0.5	-1	0	+1
Particle size (microns), E	100	200	300	-1	0	+1

**Table 2. Results of Bulk density, Moisture content, pH, and LOI**

Clay type	Bulk density (g/ml)	% moisture content	pH	LOI (%)
Ngbo clay	1.25	3.33	7.5	10.52

### 3.2 Characterization of Raw Clay and Pillarred Activated Clay

The chemical properties of the raw Ngbo clay was analysed using XRF and SEM.

The result of the XRF composition analysis of raw Ngbo clay and Pillarred activated Ngbo clay (PLC) is presented in Table 4. The result showed that raw and activated clays have contaminations of oxides and other impurities, but the clay minerals compositions are not meaningfully affected by thermal treatments even under strong conditions and below 50 °C as reported in literature by [25,26] and [27]. This shows that improvement on the properties of the clay by chemical methods below 500 °C is difficult due to its low reactivity. This result of the XRF on the Ngbo raw clay and pillarred activated Ngbo clays as shown in table 4 also indicates high content of silicon and aluminium oxides compared to other oxides.

The SEM image results of the raw clay at 80 $\mu$ m, 20 $\mu$ m and 8 $\mu$ m magnifications are presented in Fig. 1. The SEM image results of Ngbo raw clay showed cracking or peeling morphology and presence of tubular or rod material attributed to halloysite, clinocllore, mica and muscovites as reported in literature by [28]. The results are in agreement with the XRD results.

The SEM image results of Ngbo Pillarred activated clay at 80  $\mu$ m, 20  $\mu$ m and 8  $\mu$ m magnifications are presented in Fig. 2. The SEM image results shows retention of kaolinite structure but with noticeable small aggregate particles in between the silica-alumina plate on higher magnification, an indication of impurities on the beneficiated kaolin. The halloysite phase detected in the raw clay SEM image was not in the activated clay SEM image, which is in agreement with the XRF results. The dark and bright patches witnessed in the image were attributed to the presence of imbedded chemicals and completely dried portion of the samples respectively [28].

**Table 3. Results of XRF analysis of raw Ngbo Clay and Ngbo Pillarred activated clay**

Chemical constituent	Raw clay (Wt. %)	Pillarred activated (PLC), (Wt. %)
SiO <sub>2</sub>	62.70	65.395
TiO <sub>2</sub>	1.52	1.354
Al <sub>2</sub> O <sub>3</sub>	19.70	24.562
Fe <sub>2</sub> O <sub>3</sub>	2.06	5.667
P <sub>2</sub> O <sub>3</sub>	–	0.000
CaO	0.789	0.359
MgO	0.026	0.586
Na <sub>2</sub> O	0.20	0.261
K <sub>2</sub> O	0.85	1.196
Mn <sub>2</sub> O <sub>3</sub>	–	0.148
V <sub>2</sub> O <sub>5</sub>	0.071	–
Cr <sub>2</sub> O <sub>3</sub>	0.035	0.011
CuO	0.044	–
BaO	0.19	–
L.O.I	11.82	–
SO <sub>3</sub>	–	0.220
Cl	–	0.217
ZnO	–	0.016
SrO	–	0.007

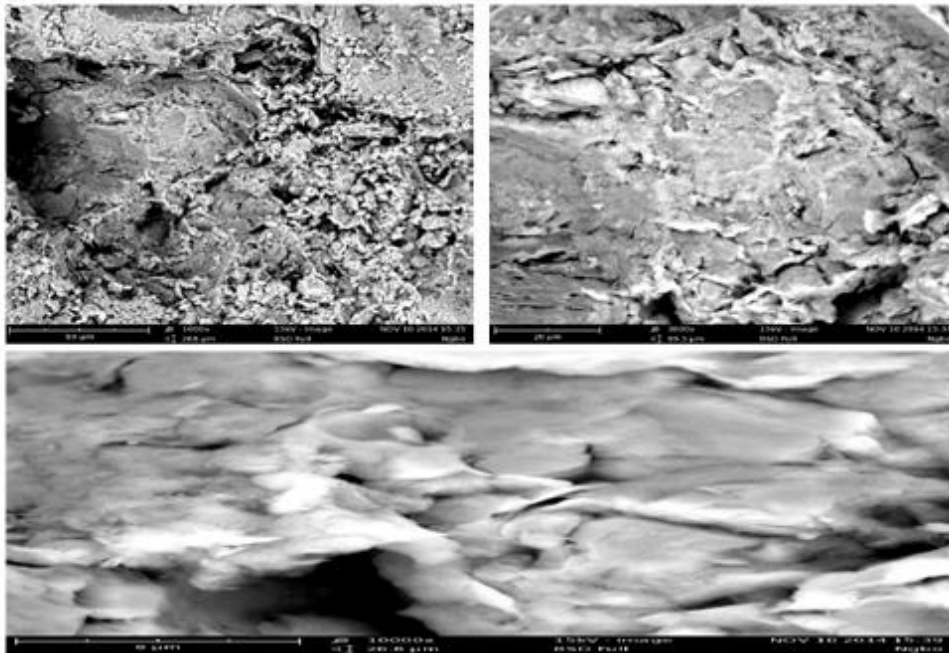


Fig. 1. Results of SEM analysis of Ngbo raw clay

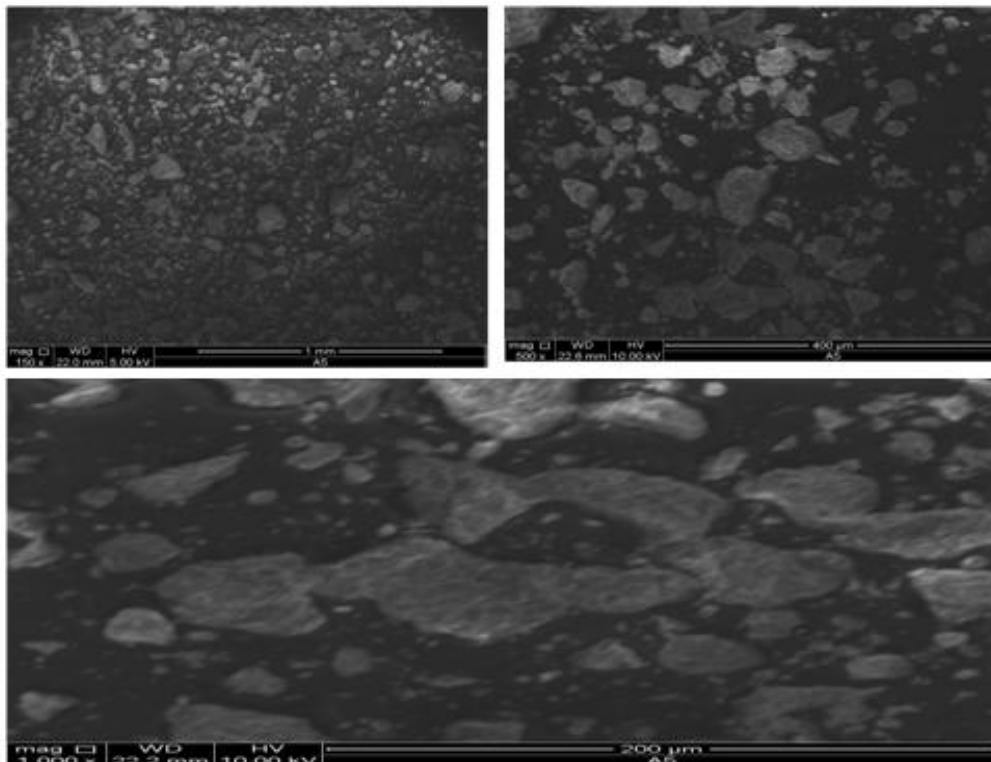


Fig. 2. Results of SEM analysis of Ngbo PLC

### 3.3 Esterification Process Results

Esterification technique was used to obtain the responses and yield of Pillarred Activated Catalyst (PLC) as shown in Table 4.

**Table 4. Result showing responses and yield of PLC**

Std	Run	Factor 1A (°C)	Factor 1B (min)	Factor 1C (ml)	Factor 1D(g)	Factor 1E (mic)	Response (ml)	Yield (%)
37	1	70	30	3.75	0.25	200	30.60	30.93
22	2	70	360	2.5	0.38	200	19.50	55.98
23	3	70	30	5	0.38	200	40.40	8.80
29	4	70	195	2.5	0.38	100	20.80	52.29
26	5	90	195	3.75	0.25	200	27.70	37.47
1	6	50	30	3.75	0.38	200	31.20	29.57
32	7	70	195	5	0.38	300	39.30	8.82
46	8	70	195	3.75	0.38	200	30.40	31.38
10	9	70	360	3.75	0.38	100	29.50	32.34
34	10	90	195	3.75	0.38	100	27.20	37.61
21	11	70	30	2.5	0.38	200	19.90	55.08
35	12	50	195	3.75	0.38	300	28.70	33.41
8	13	70	195	5	0.5	200	32.00	27.77
4	14	90	360	3.75	0.38	200	25.60	42.21
2	15	90	30	3.75	0.38	200	32.40	26.86
11	16	70	30	3.75	0.38	300	30.40	29.47
31	17	70	195	2.5	0.38	300	20.20	53.13
3	18	50	360	3.75	0.38	200	30.70	30.70
24	19	70	360	5	0.38	200	38.40	13.32
16	20	90	195	5	0.38	200	37.00	16.48
44	21	70	195	3.75	0.38	200	30.40	31.38
12	22	70	360	3.75	0.38	300	29.50	31.55
36	23	90	195	3.75	0.38	300	28.10	34.80
17	24	70	195	3.75	0.25	100	30.90	29.13
18	25	70	195	3.75	0.5	100	30.60	29.82
45	26	70	195	3.75	0.38	200	30.80	30.47
33	27	50	195	3.75	0.38	100	32.20	26.15
25	28	50	195	3.75	0.25	200	32.00	27.77
20	29	70	195	3.75	0.5	300	30.60	29.00
27	30	50	195	3.75	0.5	200	31.70	28.44
30	31	70	195	5	0.38	100	40.00	8.26
42	32	70	195	3.75	0.38	200	30.80	30.47

Std	Run	Factor 1A (°C)	Factor 1B (min)	Factor 1C (ml)	Factor 1D(g)	Factor 1E (mic)	Response (ml)	Yield (%)
41	33	70	195	3.75	0.38	200	31.00	30.02
39	34	70	30	3.75	0.5	200	31.10	29.80
6	35	70	195	5	0.25	200	24.00	45.82
43	36	70	195	3.75	0.38	200	30.40	31.38
38	37	70	360	3.75	0.25	200	29.80	32.73
19	38	70	195	3.75	0.25	300	30.30	29.70
40	39	70	360	3.75	0.5	200	29.40	33.63
7	40	70	195	2.5	0.5	200	19.50	55.98
28	41	90	195	3.75	0.5	200	28.00	36.79
14	42	90	195	2.5	0.38	200	17.30	60.95
5	43	70	195	2.5	0.25	200	19.50	55.98
13	44	50	195	2.5	0.38	200	21.00	52.60
9	45	70	30	3.75	0.38	100	31.40	27.98
15	46	50	195	5	0.38	200	42.50	4.06

### 3.4 Analysis of Variance (ANOVA) for Pillared Clay (PLC)

The result of the ANOVA for Pillared Clay (PLC) is shown in table 5. The result showed that RSM model is significant of the experimental results as indicated from the F – value of 143.88 calculated and very low probability value of P <0.0001. The lack of fit F – value of 8.71 showed that it was significant and there is 23.07% chance that a Lack of Fit F – value this large could occur due to noise. The significant terms of the model was determined by F- value and P- values. The values of “Prob > F” less than 0.0500 indicate the model terms are significant while values greater than 0.100 indicate that the model terms are not significant. ANOVA involves subdividing the total variation of a set of data onto component parts. The F – value is defined as the ratio of the mean square of regression (MRR) to the error (MRe). The smaller the magnitude of the F – value, the more significant is the corresponding coefficient [29]. If P – value of lack of fit is less than 0.05, there is statistically significant lack of fit at 95% confidence level [30].

However, the result in table 5 indicates that the significant model terms A, B, C, AB and C<sup>2</sup>, which implies that only linear effects of temperature, process duration, excess reactants, interactive effects of temperature and process duration and quadratic effects of excess reactant were significant. The model accuracy was confirmed by the correlation coefficient of the regression model which is 0.8674. The correlation coefficient showed that 86.74% of the total variation in the final concentration was attributed to the experimental variables considered in this study. The high value of the R<sup>2</sup>

and the “Pred R-Squared” of 0.8236 is in good agreement with the “Adj R – Squared” of 0.9192 as reported in literature by [29].

The standard deviation for the model was 6.48, which indicated that the predicted values are still considered suitable to correlate the experimental data. “Adeq Precision” measures the signal to noise ratio. A ratio greater than 4 is desirable. Here it has a ratio of 11.341, which indicates an adequate signal.

The Final equation in terms of coded factors gives:

$$\text{Yield} = + 30.85 + 3.78A + 2.12B - 19.29C - 1.14D + 0.39E + 3.56AB + 1.02AC - 0.34AD - 2.52AE + 0.92BC + 0.51BD - 0.57BE - 4.51CD - 0.070CE - 0.35DE + 0.62A^2 - 0.62B^2 + 4.74C^2 + 3.53D^2 - 2.08E^2.$$

The coefficient with one factor represents the effect of the particular factor, while the coefficients with two factors and those with second order terms represent the interaction between two factors and quadratic effect respectively (Mohd and Rasyidah 2010).

Final model equation after eliminating the insignificant terms in terms of coded variables:

$$\text{Yield} = + 30.85 + 3.78A - 19.29C + 4.74C^2.$$

The regression model developed was further assessed using residual plots as shown in Fig. 3-6. Residual is the difference between the experimental value and value predicted by the model. This tests the assumption of constant variance of the experimental data.

**Table 5. ANOVA table for Pillared Clay (PLC)**

Source	Sum of Squares	Df	Mean Square	F – Value	P – Value Prob > F
Model	6864.87	20	343.24	8.18	<0.0001 significant
A – Temperature	228.54	1	228.54	5.44	0.0280
B – Process duration	71.91	1	71.91	1.71	0.2025
C – Excess reactant	5952.5	1	5952.51	141.80	< 0.0001
D – Effect of Catalyst	20.93	1	20.93	0.50	0.4866
E – Particle size	2.48	1	2.48	0.059	0.8099
AB	50.55	1	50.55	1.20	0.2829
AC	4.14	1	4.14	0.099	0.7561
AD	0.46	1	0.46	0.011	0.9179
AE	25.35	1	25.35	0.60	0.4444
BC	3.37	1	3.37	0.080	0.7793
BD	1.03	1	1.03	0.025	0.8768
BE	1.30	1	1.30	0.031	0.8618



Source	Sum of Squares	Df	Mean Square	F – Value	P – Value Prob > F
CD	81.45	1	81.45	1.94	0.1759
CE	0.020	1	0.020	4.669E-004	0.9829
DE	0.48	1	0.48	0.012	0.9154
A <sup>2</sup>	3.40	1	3.40	0.081	0.7784
B <sup>2</sup>	3.39	1	3.39	0.081	0.7785
C <sup>2</sup>	196.13	1	196.13	4.67	0.0404
D <sup>2</sup>	108.84	1	108.84	2.59	0.1199
E <sup>2</sup>	37.64	1	37.64	0.90	0.3527
Residual	1049.49	25	41.98		
Lack of fit	1047.67	20	52.38	143.88	< 0.0001 significant
Pure Error	1.82	5	0.36		
Cor Total	7914.36	45			

### 3.4.1 Residual plots for PLC

The residual plots are shown in Fig. 3 – Fig. 6. The trends of the residual plots indicate that the model can be considered as a good fit and that the regression equations follow the experimental results with a good accuracy. The plots indicate values that are not easily predicted by the model.

The plot of residuals against run checks for lurking variables that may have influenced the response during the experiment. The normal plot of residuals indicates whether the residuals follow a normal distribution, and the plot of predicted against actual response values helps to detect a value, group of values that are not easily predicted by the model.

Design-Expert® Software  
Yield

Color points by value of Yield:  
60.95  
4.06

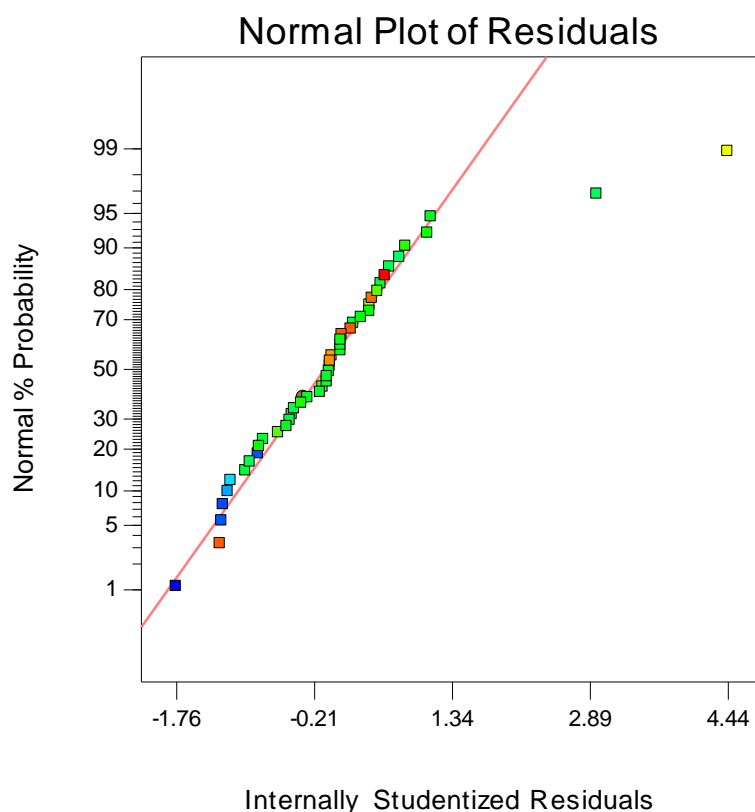


Fig. 3. Normal plot of residuals for PLC

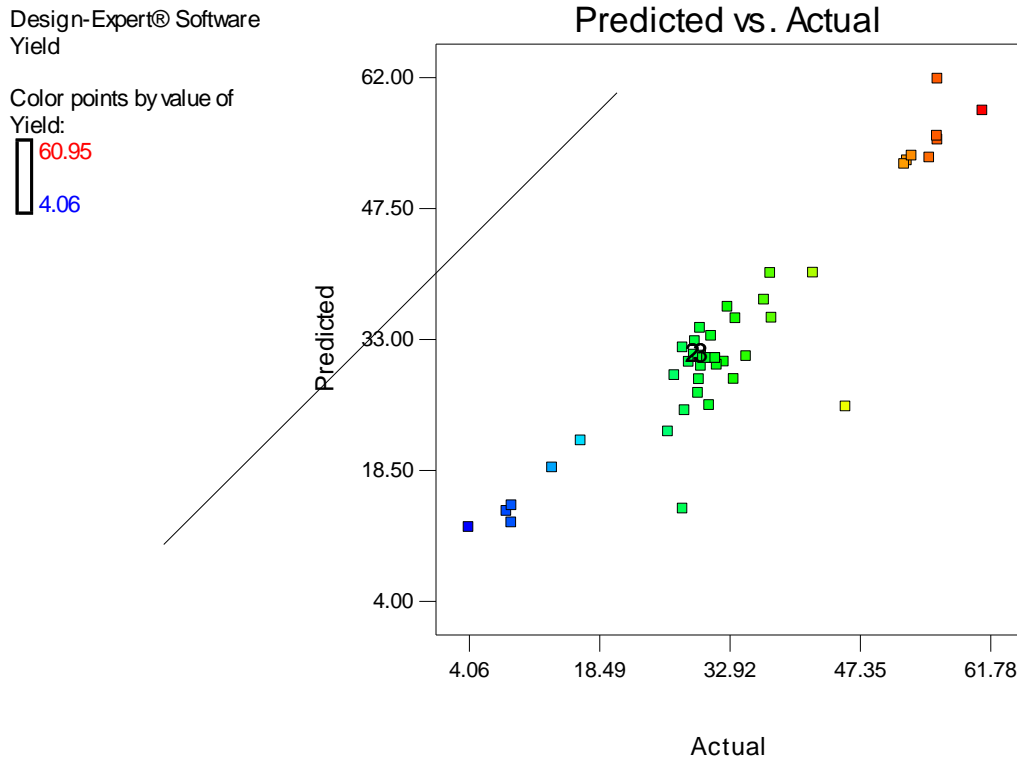


Fig. 4. Plot of predicted verse actual for PLC

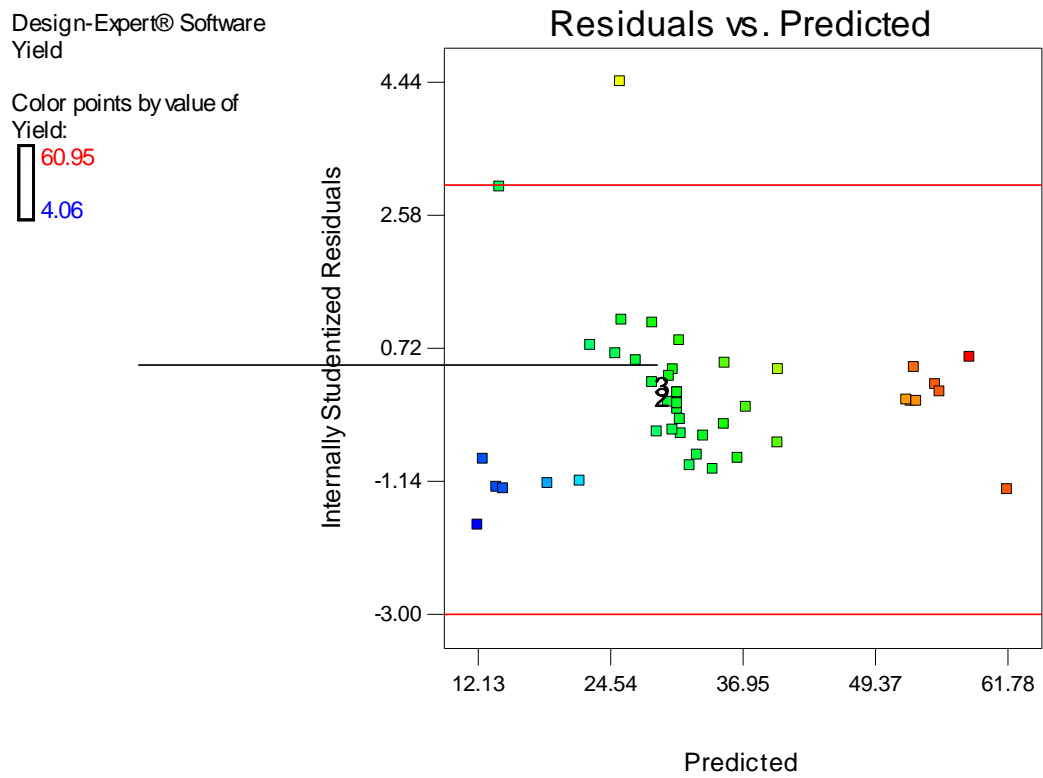


Fig. 5. Plot of residuals verse predicted for PLC

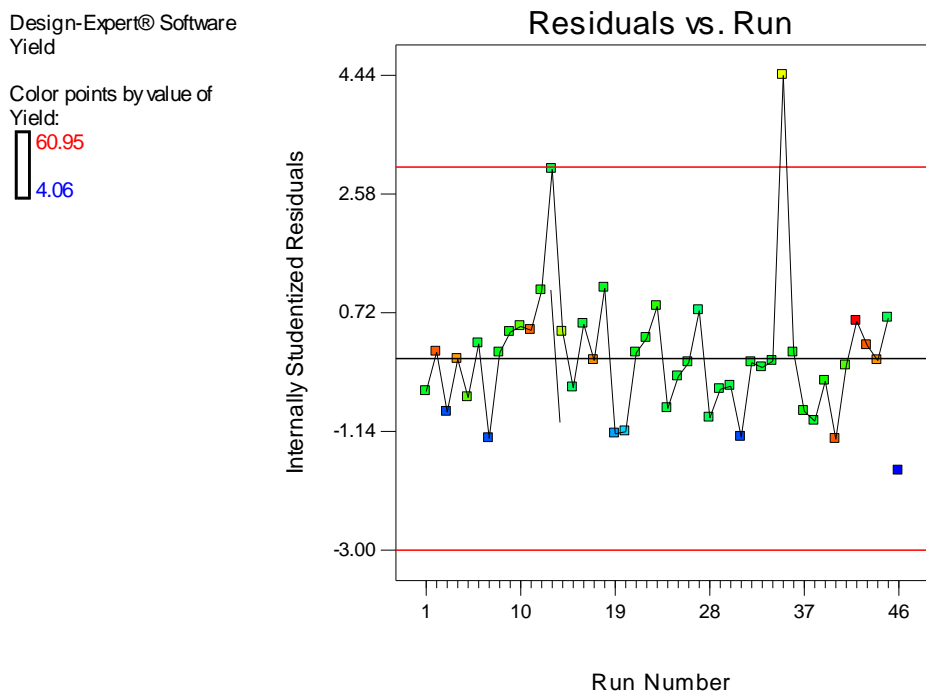


Fig. 6. Plot of residuals verse run for PLC

### 3.4.2 Contour plots for PLC

The contour plots for PLC are shown in Fig. 7 to Fig. 16. The circular nature of the contour plots signifies that the interactive effects between the variables are not significant and the optimum

values of the test process variables cannot be easily obtained [31,29]. The non circular nature of the contour plots reveals that there is an interaction between the process variables studied and the optimum value of the process variables can be easily obtained.

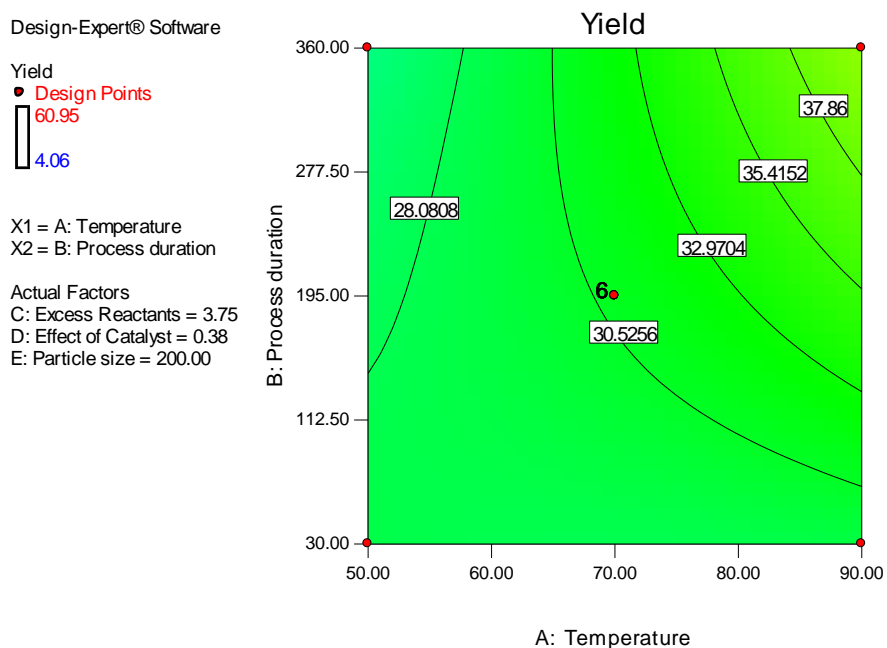


Fig. 7. The contour plots for process duration against Temperature and yield of PLC

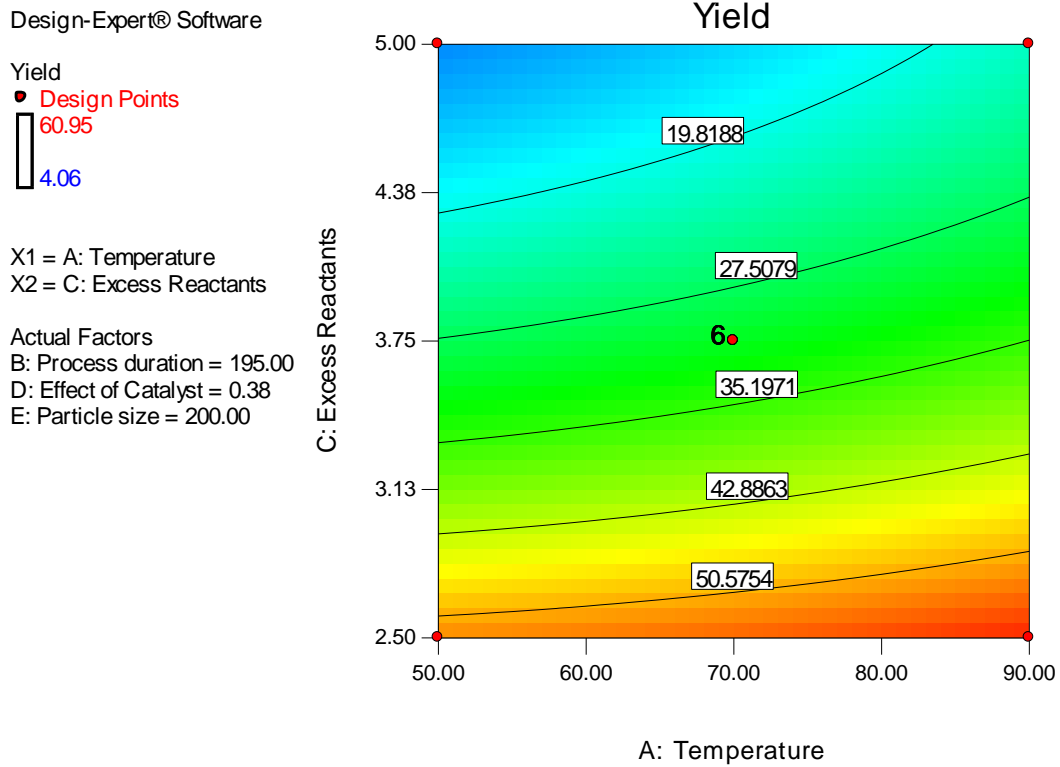


Fig. 8. The contour plots for excess reactants against Temperature and yield of PLC

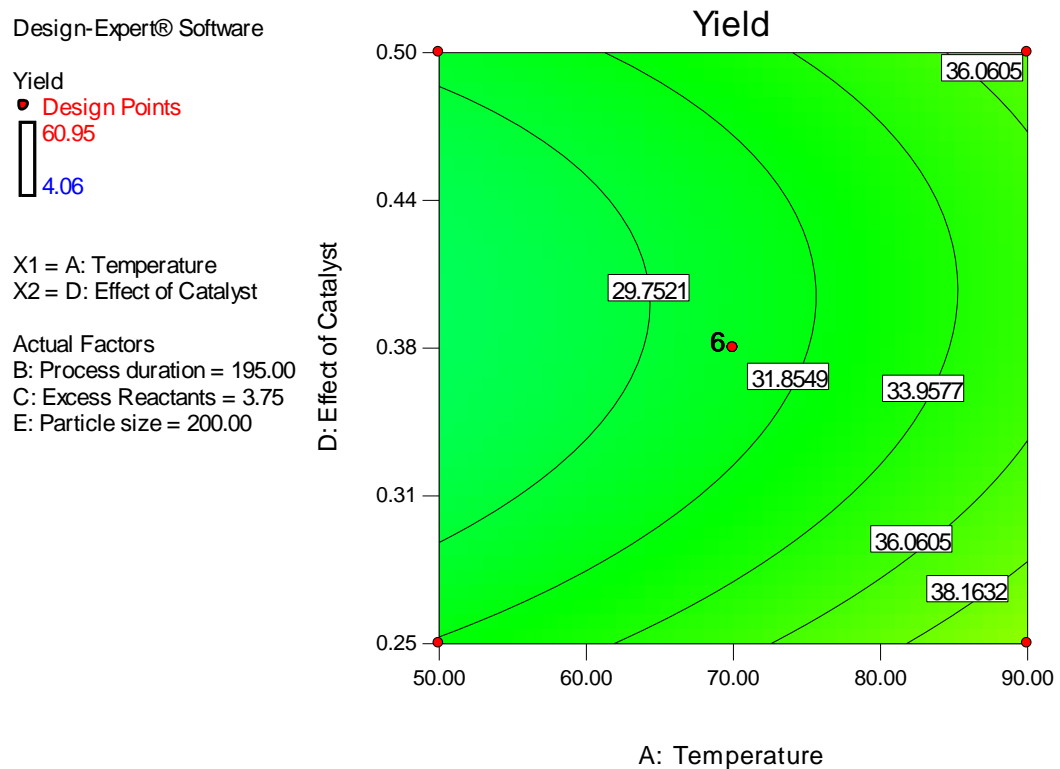


Fig. 9. The contour plots for effect of catalyst against Temperature and yield of PLC

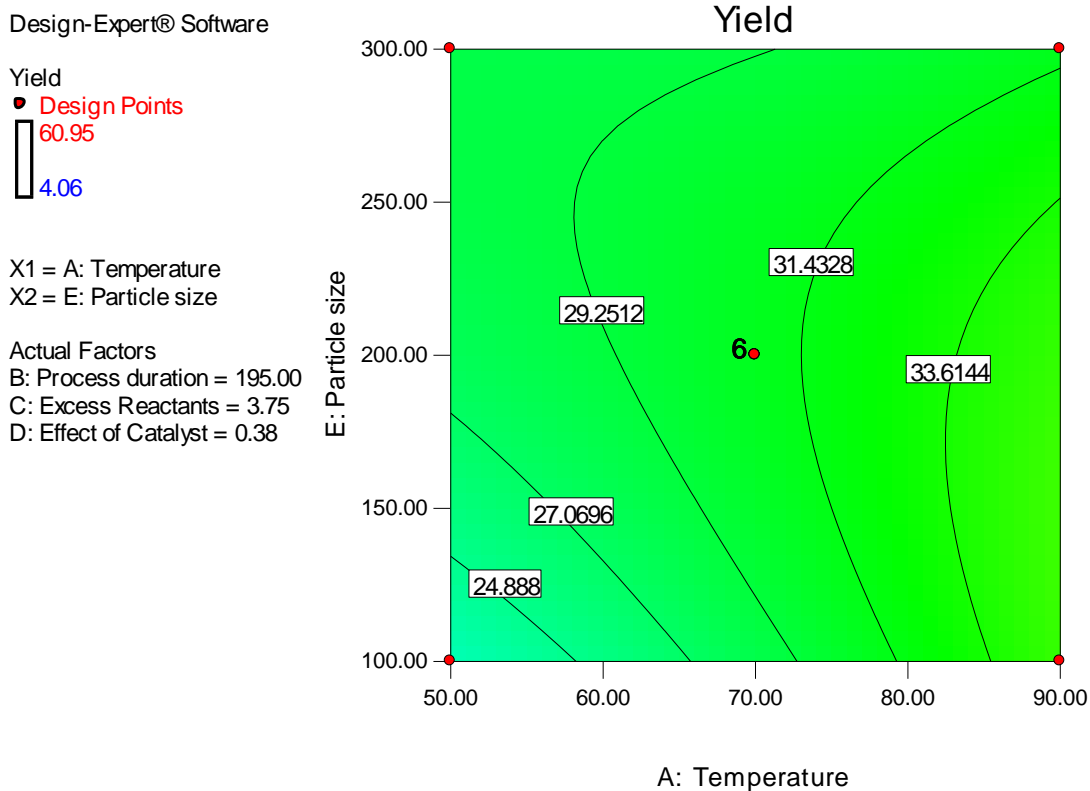


Fig. 10. The contour plots for excess reactants against Temperature and yield of PLC

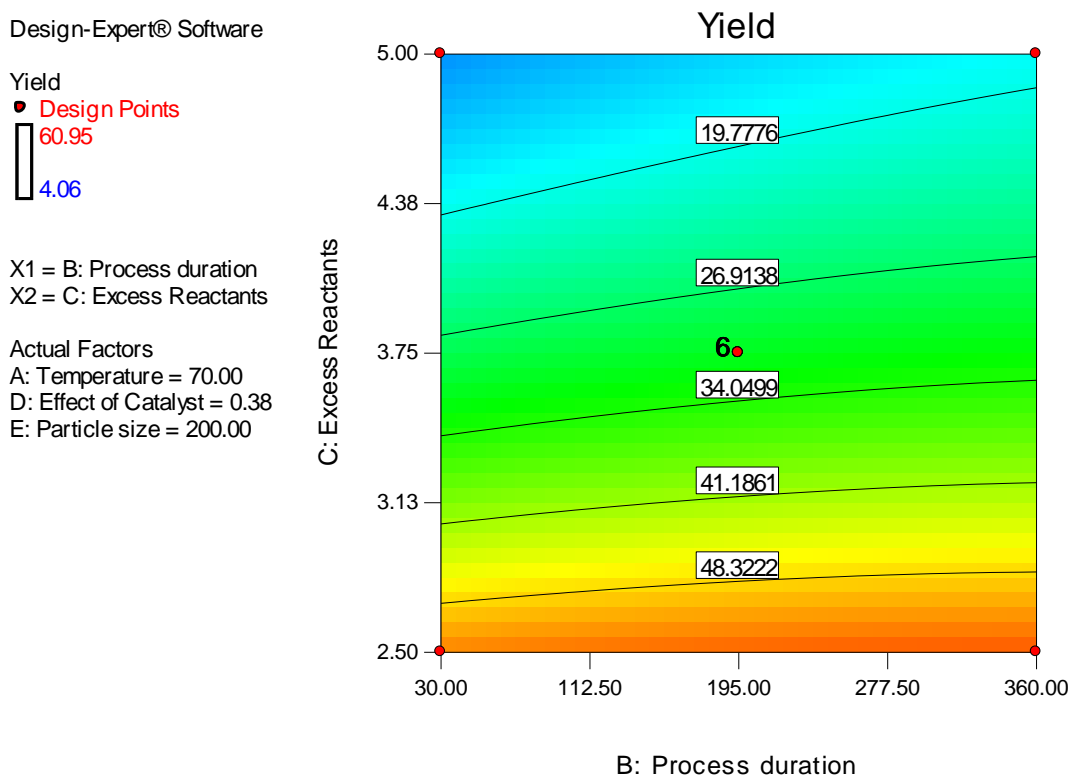


Fig. 11. The contour plots for excess reactants against process duration and yield of PLC

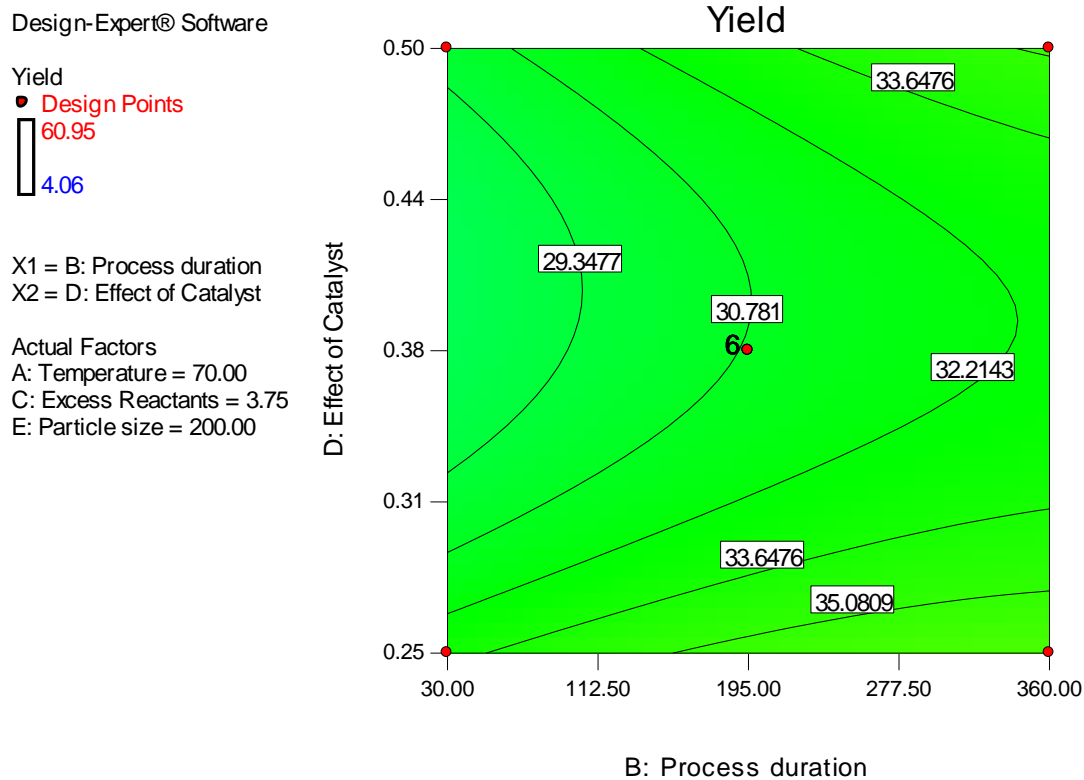


Fig. 12. The contour plots for effect of catalyst against process duration and yield of PLC

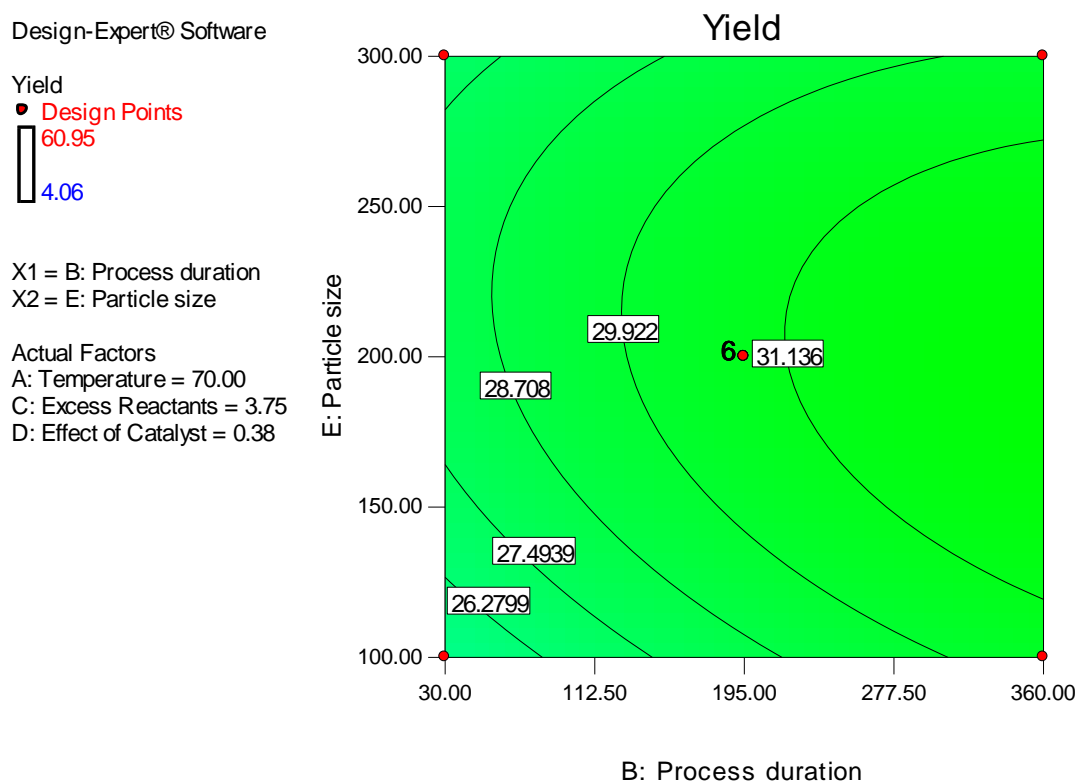


Fig. 13. The contour plots for particle size against process duration and yield of PLC

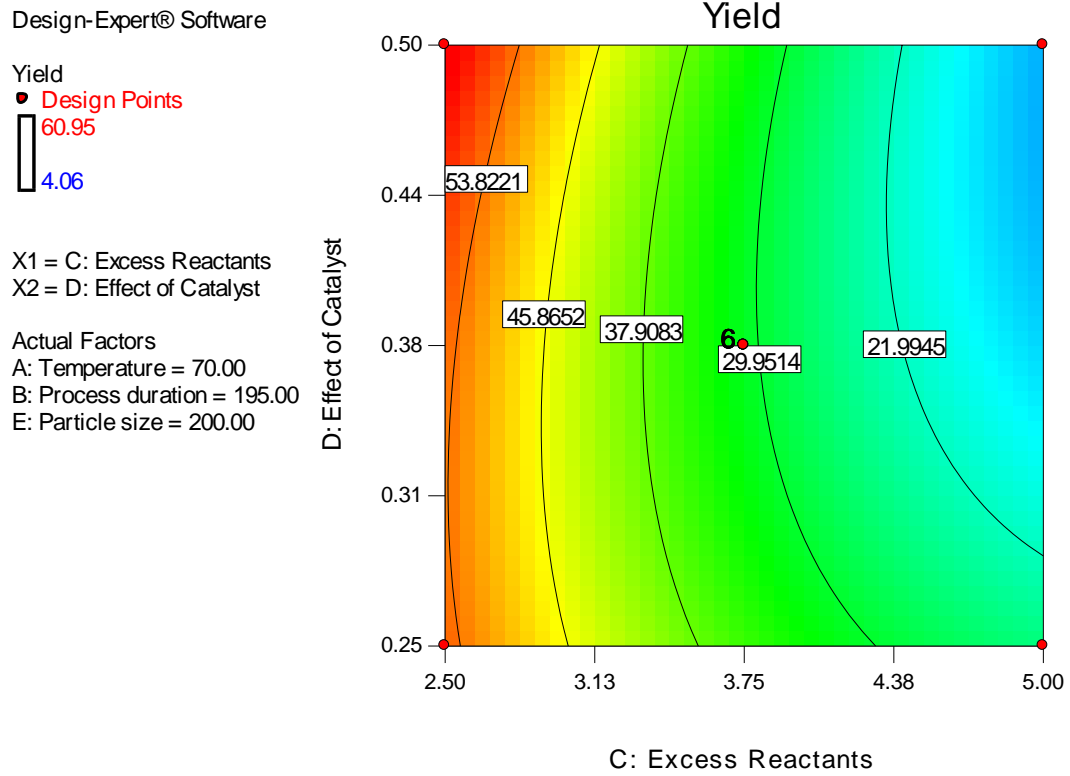


Fig. 14. The contour plots for effect of catalyst against excess reactants and yield of PLC

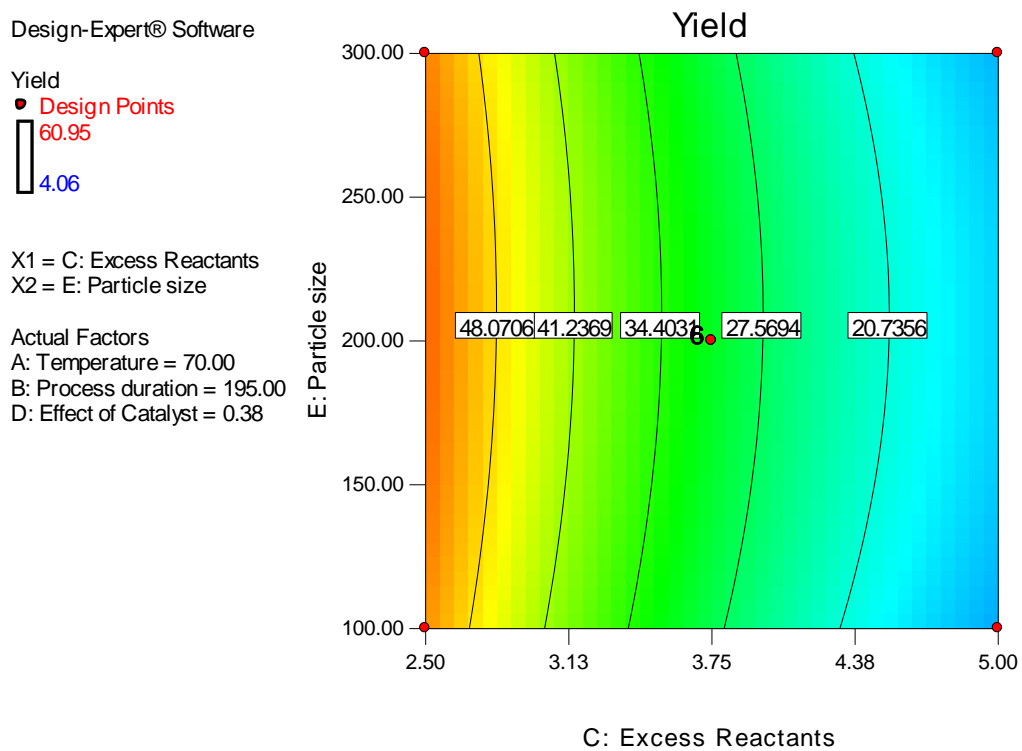


Fig. 15. The contour plots for particle size against excess reactants and yield of PLC

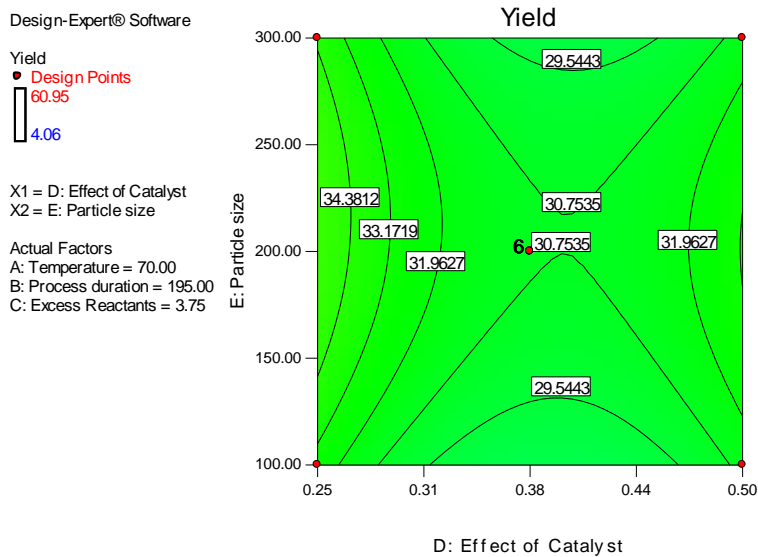


Fig. 16. The contour plots for particle size against effect of catalyst and yield of PLC

### 3.4.3 The 3 - D Plot for PLC

The 3 – Dimensional plots of the response surface model are shown in Figs. 17 to 26. The results showed that the optimum value of the conversion was 42 for the process variables studied; which are similar to results obtained by [29,23,24,30]. The excess reactants increases with process duration as the yield also increases. The response surface plots showed clear peaks, implying that the maximum values of the response were attributed to the factors in the design space. The three-dimensional surfaces

provide useful information about the behavior of the system within the experiment design, facilitate an examination of the effects of the experimental factors on the responses and contour plots between the factors [31,34,35]. The 3-D plots were generated by continually varying any two variables while maintaining all other input variables constant at their null point. The 3-D curves were observed to have elliptical nature with any two concerned variables. This denotes that the quadratic model chosen was appropriate with significant correlation between the two variables [36,37].

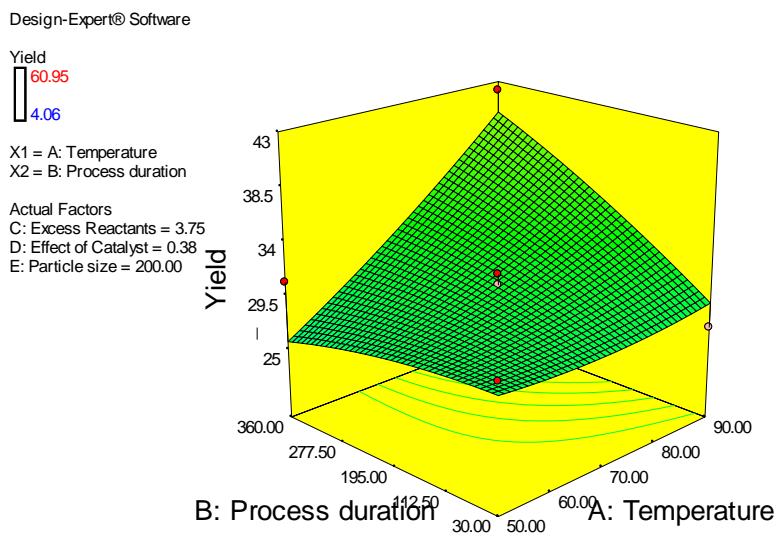


Fig. 17. The 3 - D Plot for process duration against temperature and yield of PLC



Design-Expert® Software

Yield  
█ 60.95  
█ 4.06

X1 = A: Temperature  
 X2 = C: Excess Reactants

Actual Factors  
 B: Process duration = 195.00  
 D: Effect of Catalyst = 0.38  
 E: Particle size = 200.00

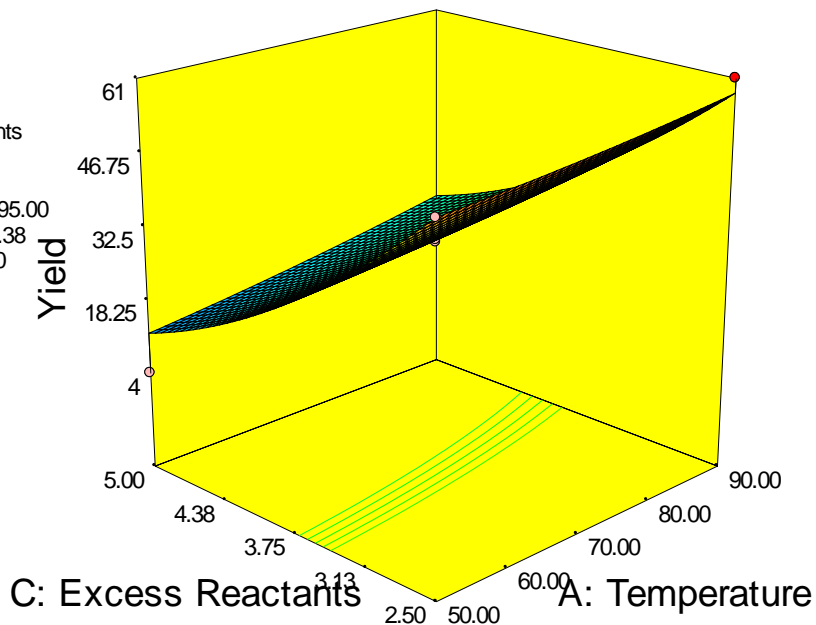


Fig. 18. The 3 - D Plot for excess reactants against temperature and yield of PLC

Design-Expert® Software

Yield  
█ 60.95  
█ 4.06

X1 = A: Temperature  
 X2 = D: Effect of Catalyst

Actual Factors  
 B: Process duration = 195.00  
 C: Excess Reactants = 3.75  
 E: Particle size = 200.00

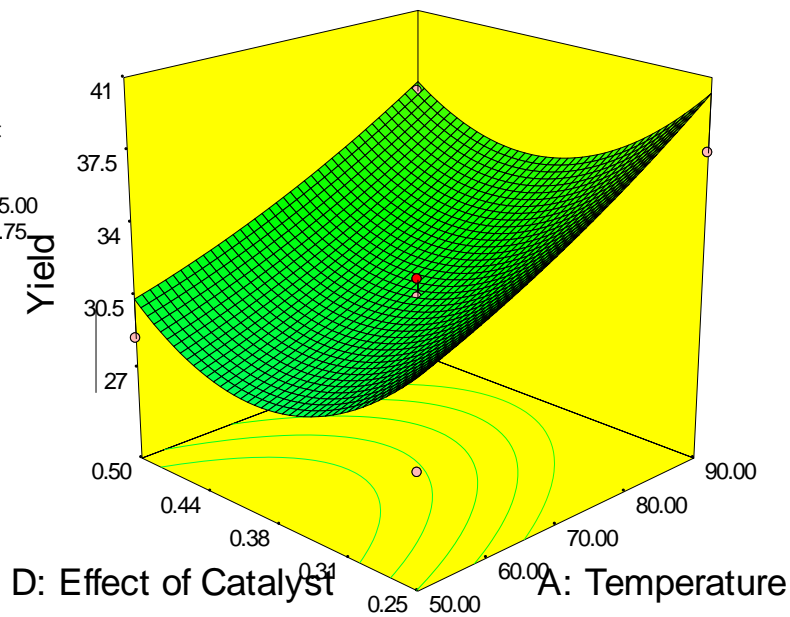


Fig. 19. The 3 - D Plot for effect of catalyst against temperature and yield of PLC

Design-Expert® Software

Yield  
 60.95  
 4.06

X1 = A: Temperature  
 X2 = E: Particle size

Actual Factors  
 B: Process duration = 195.00  
 C: Excess Reactants = 3.75  
 D: Effect of Catalyst = 0.38

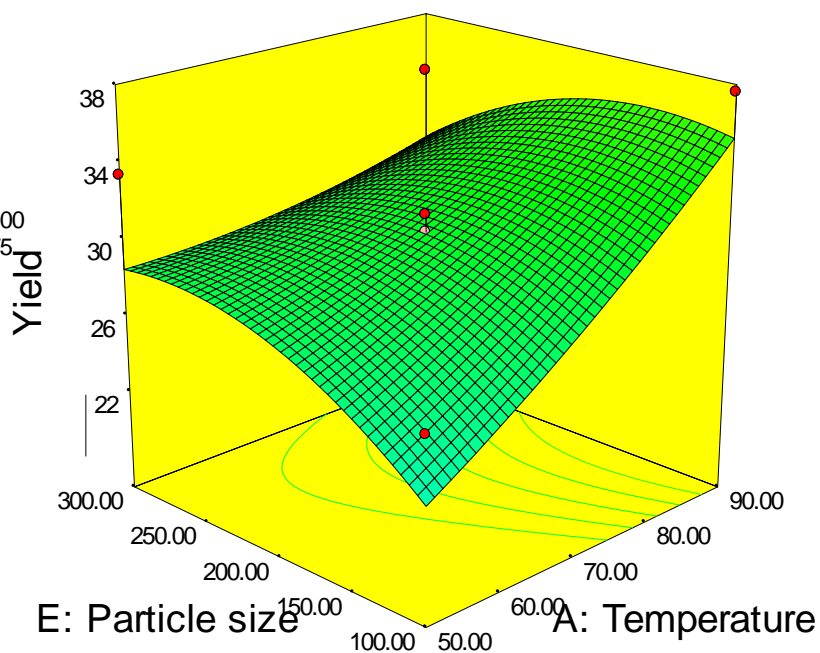


Fig. 20. The 3 - D Plot for particle size against temperature and yield of PLC

Design-Expert® Software

Yield  
 60.95  
 4.06

X1 = B: Process duration  
 X2 = C: Excess Reactants

Actual Factors  
 A: Temperature = 70.00  
 D: Effect of Catalyst = 0.38  
 E: Particle size = 200.00

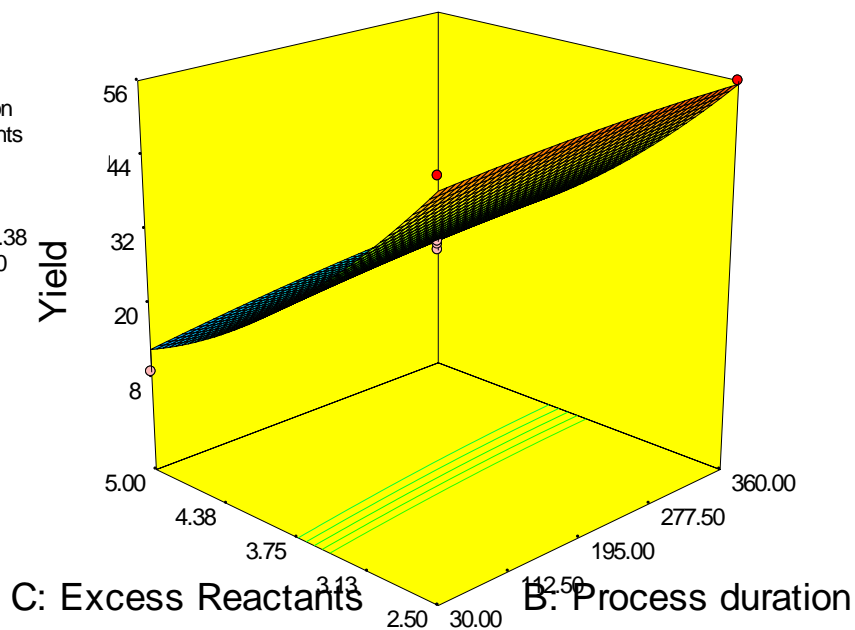


Fig. 21. The 3 - D Plot for excess reactants against duration and yield of PLC

Design-Expert® Software

Yield  
60.95  
4.06

X1 = B: Process duration  
 X2 = D: Effect of Catalyst

Actual Factors  
 A: Temperature = 70.00  
 C: Excess Reactants = 3.75  
 E: Particle size = 200.00

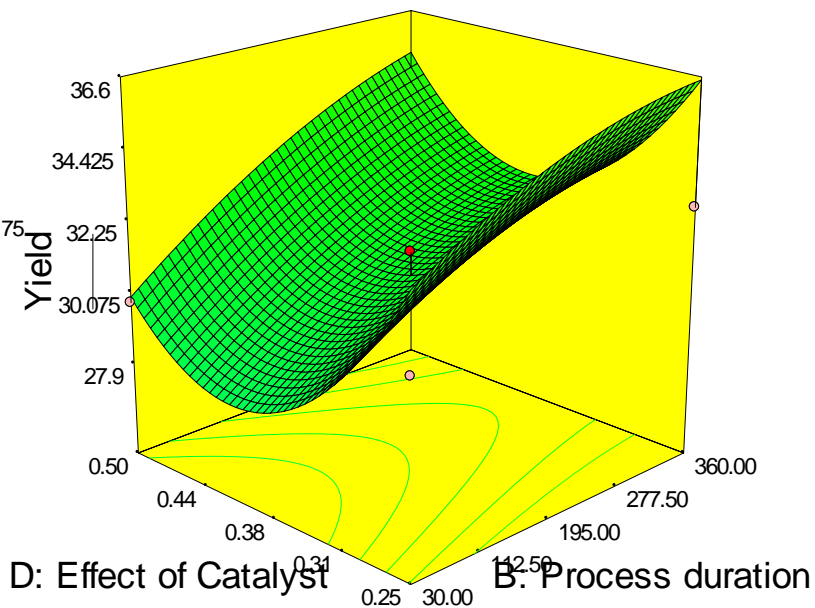


Fig. 22. The 3 - D Plot for effect of catalyst against process duration and yield of PLC

Design-Expert® Software

Yield  
60.95  
4.06

X1 = B: Process duration  
 X2 = E: Particle size

Actual Factors  
 A: Temperature = 70.00  
 C: Excess Reactants = 3.75  
 D: Effect of Catalyst = 0.38

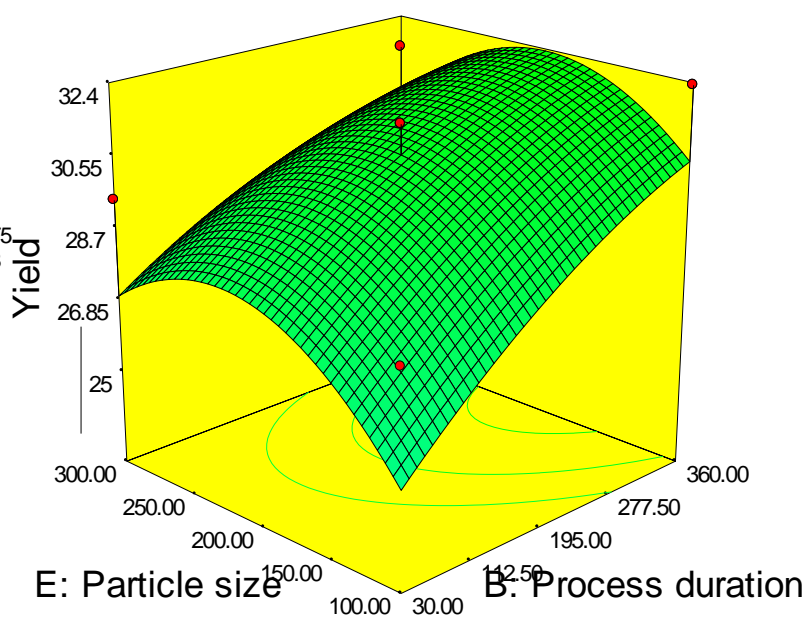


Fig. 23. The 3 - D Plot for particle size against process duration and yield of PLC

Design-Expert® Software

Yield  
 60.95  
 4.06

X1 = C: Excess Reactants  
 X2 = D: Effect of Catalyst

Actual Factors  
 A: Temperature = 70.00  
 B: Process duration = 195.00  
 E: Particle size = 200.00

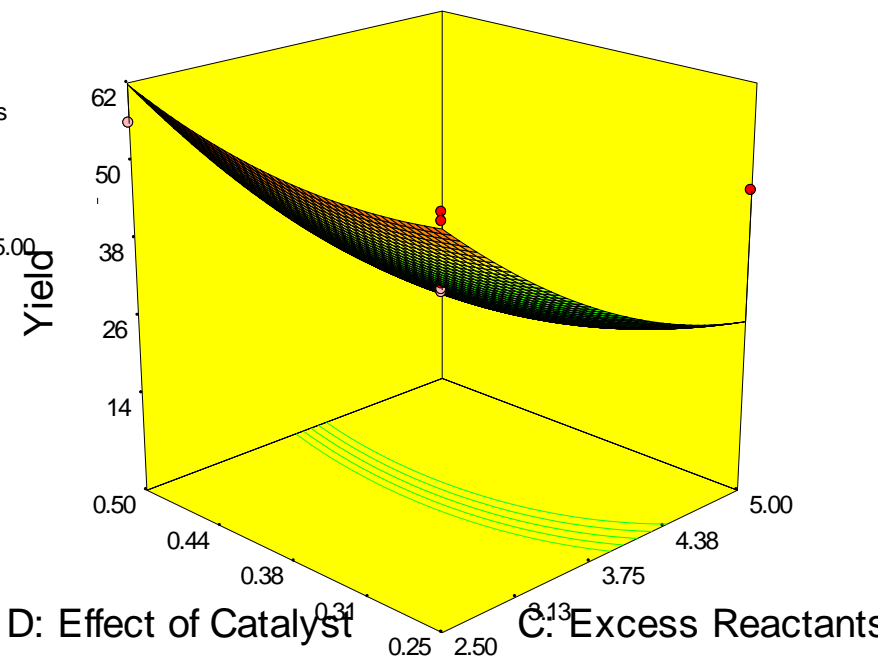


Fig. 24. The 3 - D Plot for effect of catalyst against excess reactants and yield of PLC

Design-Expert® Software

Yield  
 60.95  
 4.06

X1 = C: Excess Reactants  
 X2 = E: Particle size

Actual Factors  
 A: Temperature = 70.00  
 B: Process duration = 195.00  
 D: Effect of Catalyst = 0.38

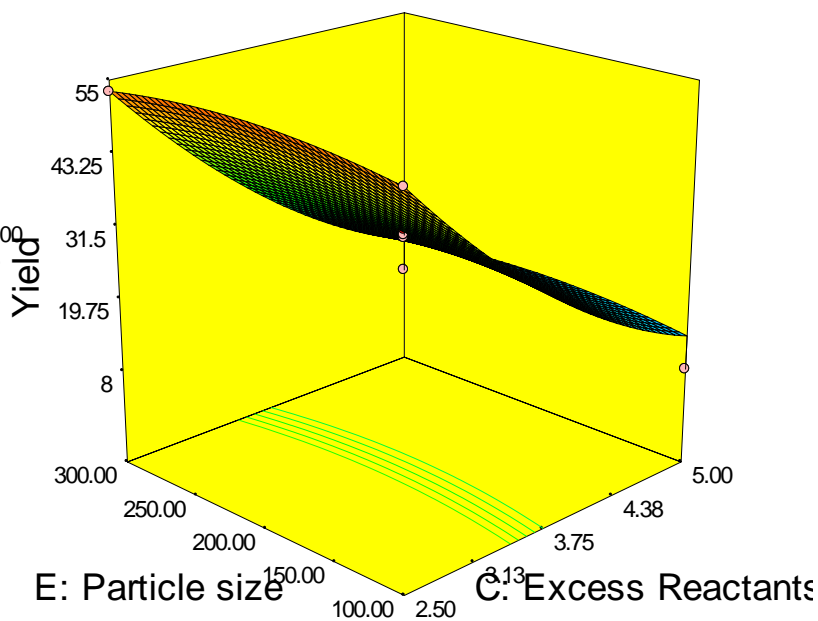
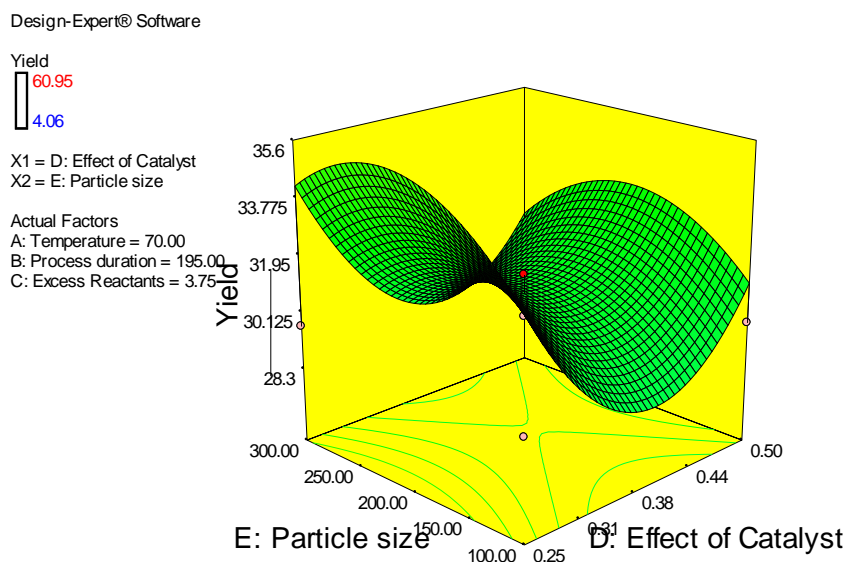


Fig. 25. The 3 - D Plot for particle size against excess reactants and yield of PLC



**Fig. 26. The 3 - D Plot for particle size against effect of catalyst and yield of PLC**

### 3.4.4 Process optimization

In the process optimization for PLC at Table 6, desirability function was used to obtain the optimum value. The time and temperature were set at minimum while the catalyst weight, particle size and excess reactant were set in range. The conversion yield was set at maximum. The optimum process conditions for the variables were 359.93 min, 90°C, 4.40ml, 0.50g, and 299.92 microns for time, temperature, excess reactant, catalyst weight and particle size respectively. The predicted conversion yield was 27.5361. The optimization was validated at those experimental conditions and conversion yield of 45.65 was obtained.

**Table 6. Validation of optimization results**

Catalysts	Model Desirability	Temp (°C)	Time (min)	Excess Reactant (ml)	Catalyst Weight (g)	Particle Size (microns)	Yield (ml)	% Conversion	% Error
PLC	27.5361	90	359.93	4.40	0.50	299.92	25.00	45.65	2.54

The summary of the model validation for the catalyst produced (PLC) is shown in table 6. The result indicates that Ngbo PLC is a good catalyst produced when compared to other catalyst produced from Ngbo as a result of its less percentage error and its pH being alkaline.

## 4. CONCLUSIONS

The study presented the optimum conditions for esterification reaction of acetic acid and ethanol using Ngbo pillared activated clay catalyst. The optimum conditions for esterification reaction for the process conditions of temperature, time duration, amount of reactant, catalyst weight and particle size was determined using Response

Surface Methodology (RSM) approach. The optimum process conditions for the variables studied for time, temperature, excess reactant, catalyst weight and particle size were 359.93 min, 90°C, 4.40ml, 0.50g, and 299.92 microns respectively. The maximum predicted esterification yield was 27.5361. The XRF analysis showed that the clay was made of mainly SiO<sub>2</sub> and aluminium while SEM results indicated crystalline nature suitable for esterification. The model validation showed that the experimental value obtained at the optimal conditions was in good agreement with the values predicted from the model with relatively small error of 2.54% between them. The predicted and experimental values from the

model showed less than 5% difference thereby making the Box-Behnken design approach an efficient, effective and reliable method for the esterification of acetic acid and ethanol using Ngbo Pillarred activated clay catalyst.

## DISCLAIMER

The products used for this research are commonly and predominantly use products in our area of research and country. There is absolutely no conflict of interest between the authors and producers of the products because we do not intend to use these products as an avenue for any litigation but for the advancement of knowledge. Also, the research was not funded by the producing company rather it was funded by personal efforts of the authors.

## ACKNOWLEDGEMENT

The authors gratefully acknowledge Food Science and Technology Department's Biochemistry Laboratory at Ebonyi State University, Ebonyi State, Nigeria for all their facilities used throughout the research work.

## COMPETING INTERESTS

Authors have declared that no competing interests exist.

## REFERENCES

- Reddy CR, Iyengar P, Nagendrappa G, Prakash BS. Esterification of dicarboxylic acids to diesters over Mn<sup>+</sup>-montmorillonite clay catalysts. *Catalysis letters*. 2005;101(1):87-91.
- Chen CC, Hayes KF. X-ray absorption spectroscopy investigation of aqueous Co (II) and Sr (II) sorption at clay-water interfaces. *Geochimica et Cosmochimica Acta*. 1999;63(19-20):3205-15.
- Yadav GD, Thathagar MB. Esterification of maleic acid with ethanol over cation-exchange resin catalysts. *Reactive and Functional polymers*. 2002;52(2):99-110.
- Zhang Y, Ma L, Yang J. Kinetics of esterification of lactic acid with ethanol catalyzed by cation-exchange resins. *Reactive and Functional Polymers*. 2004;61(1):101-14.
- Kirumakki SR, Nagaraju N, Chary KV. Esterification of alcohols with acetic acid over zeolites H $\beta$ , HY and HZSM5. *Applied Catalysis A: General*. 2006;299:185-92.
- Kirumakki SR, Nagaraju N, Narayanan S. A comparative esterification of benzyl alcohol with acetic acid over zeolites H $\beta$ , HY and HZSM5. *Applied Catalysis A: General*. 2004;273(1-2):1-9.
- Wu KC, Chen YW. An efficient two-phase reaction of ethyl acetate production in modified ZSM-5 zeolites. *Applied Catalysis A: General*. 2004;257(1):33-42.
- Chu W, Yang X, Ye X, Wu Y. Vapor phase esterification catalyzed by immobilized dodecatungstosilicic acid (SiW<sub>12</sub>) on activated carbon. *Applied Catalysis A: General*. 1996;145(1-2):125-40.
- Sepulveda JH, Yori JC, Vera CR. Repeated use of supported H<sub>3</sub>PW<sub>12</sub>O<sub>40</sub> catalysts in the liquid phase esterification of acetic acid with butanol. *Applied Catalysis A: General*. 2005;288(1-2):18-24.
- Jermy BR, Pandurangan A. Catalytic application of Al-MCM-41 in the esterification of acetic acid with various alcohols. *Applied Catalysis A: General*. 2005;288(1-2):25-33.
- Kirumakki SR, Nagaraju N, Chary KV, Narayanan S. Kinetics of esterification of aromatic carboxylic acids over zeolites H $\beta$  and HZSM5 using dimethyl carbonate. *Applied Catalysis A: General*. 2003;248(1-2):161-7.
- Nwabanne JT, Onu CE, Nwankwokuw OC. Equilibrium, kinetics and thermodynamics of the bleaching of palm oil using activated nando clay. *Journal of Engineering Research and Reports*. 2018;1(3):1-3.
- Ajemba RO, Onukwuli OD. Process optimization of sulphuric acid leaching of alumina from Nteje clay using central composite rotatable design. *International Journal of Multidisciplinary Sciences and Engineering*. 2012;3(5):1-7.
- Onu CE, Nwabanne JT. Application of response surface methodology in malachite green adsorption using Nteje clay. *Open J. Chem. Eng. Sci*. 2014;1(2):19-33.
- Nnenna NV, Philomena KI, Elijah OC. Removal of Methylene Blue Dye from Aqueous Solution Using Modified Ngbo Clay.
- Elijah OC, Nwabanne JT. Adsorption studies on the removal of Eriochrome black-T from aqueous solution using Nteje clay. *SOP Trans. Appl. Chem*. 2014;1(2):14-25. DOI: 10.15764/EH.2014.02015

17. Ike IS, Asadu CO, Ezema CA, Onah TO, Ogbodo NO, Godwin-Nwakwasi EU, Onu CE. ANN-GA, ANFIS-GA and Thermodynamics base modeling of crude oil removal from surface water using organic acid grafted banana pseudo stem fiber. *Applied Surface Science Advances*. 2022 Jun 1;9:100259. DOI: <https://doi.org/10.9734/AJOCS/2021/v9i419080>
18. Ijeoma UO, Josph TN, Chijioko EO. Characterization and optimization of biodiesel produced from palm oil using acidified clay heterogeneous catalyst. *Asian J. Appl. Chem. Res.* 2021;8(3):9-23. DOI: <https://doi.org/10.9734/AJACR/2021/v8i330192>
19. Ijeoma UO, Josph TN, Chijioko EO. Characterization and optimization of biodiesel produced from palm oil using acidified clay heterogeneous catalyst. *Asian J. Appl. Chem. Res.* 2021;8(3):9-23. Ijeoma UO, Josph TN, Chijioko EO. Characterization and optimization of biodiesel produced from palm oil using acidified clay heterogeneous catalyst. *Asian J. Appl. Chem. Res.* 2021;8(3):9-23. Available:<https://doi.org/10.1111/jfpp.16032>
20. Ositadinma IC, Tagbo NJ, Elijah OC. Optimum process parameters for activated carbon production from rice husk for phenol adsorption. *Current Journal of Applied Science and Technology*. 2019;36(6):1-1. DOI: [10.9734/CJAST/2019/v36i630264](https://doi.org/10.9734/CJAST/2019/v36i630264)
21. Igbokwe PK, Nwokolo SO, Ogbuagu JO. Catalytic esterification of stearic acid using a local kaolinitic clay mineral. *NJERD*. 2005;4:1.
22. Igbokwe PK, Olebunne FL. On the catalytic esterification of acetic acid with ethanol, using Nigerian montmorillonite clay: effect of reaction variables on catalyst efficiency. *Journal of the University of Chemical Technology and Metallurgy*. 2011;46(6):389-394.
23. Igbokwe PK, Ugonabo VI, Obarandiku E, Ochili A. "Characterization and use of catalyst produced from local clay resources" *Journal of Applied Sciences (JAS)*. 2008;2(2).
24. Igbokwe PK, Olebunne F, Nwakaudu M. Effect of activation parameters on conversion in clay-catalysed esterification of acetic acid. *Int. J. Basic appl. Sci.(IJBAS-IJENS)*. 2011;11(5):1-8.
25. Murat M, Amokrane A, Bastide JP, Montanaro L. Synthesis of zeolites from thermally activated kaolinite. Some observations on nucleation and growth. *Clay Minerals*. 1992;27(1):119-30.
26. Akolekar D, Chaffee A, Howe RF. The transformation of kaolin to low-silica X zeolite. *Zeolites*. 1997 Nov 1;19(5-6):359-65.
27. Demortier A, Gobeltz N, Lelieur JP, Duhayon C. Infrared evidence for the formation of an intermediate compound during the synthesis of zeolite Na-A from metakaolin. *International Journal of Inorganic Materials*. 1999;1(2):129-34.
28. Davies J, Haq S, Hawke T, Sargent JP. A practical approach to the development of a synthetic Gecko tape. *International Journal of Adhesion and Adhesives*. 2009;29(4):380-90.
29. Ejikeme PC, Ejikeme ME, BN A. RSM optimization process for uptake of water from ethanol water solution using oxidized starch. *The Pacific Journal of Science and Technology*. 2013;14:319-29.
30. Azargohar R, Dalai AK. Production of activated carbon from Luscar char: experimental and modeling studies. *Microporous and mesoporous materials*. 2005;85(3):219-25.
31. Anupam K, Dutta S, Bhattacharjee C, Datta S. Adsorptive removal of chromium (VI) from aqueous solution over powdered activated carbon: Optimisation through response surface methodology. *Chemical Engineering Journal*. 2011;173(1):135-43.
32. Igbokwe PK, Ugonabo VI, Iwegbu NA, Akachukwu PC, Olisa CJ. Kinetics of the catalytic esterification of propanol with ethanoic acid using catalyst obtained from Nigerian clays. *Journal of the University of Chemical Technology and Metallurgy*. 2008;345-348.
33. Olebunne FL, Igbokwe PK, Onyelucheya OE, Osoka EC, Ekeke IC. "Mechanistic modeling of clay-catalysed liquid-phase esterification of acetic acid". *Journal of Emerging Trends in Engineering and Applied Sciences*. 2011;2:4:631-635.
34. Panesar PS. Application of Response Surface Methodology in the Permeabilisation of Yeast Cells for Lactose Hydrolysis. *Biochem. Eng. J.* 2008;39:91-96.

35. Ahmad AA, Hameed BH. Effect of Preparation Conditions of Activated Carbon from Bamboo Waste for Real Textile Waste Water", Journal of Hazard Mater. 2010;173:487–493. Available: <http://doi.org/10.1016/j.aia.2020.04.001>
36. Onu Chijioke Elijah, Igbokwe P.K, Nwabanne J.T, Nwanjinka O.C, Ohale P.E. Evaluation of Optimization techniques in predicting optimum moisture content reduction in drying potatoe slices. Artificial intelligence in Agriculture, 2020;4:39-47. Available: <https://doi.org/10.1016/j.sajce.2020.12.003>
37. Onu C.E, Nwabanne JT, Ohale P.E, Asadu CO. Comparative analysis of RSM, ANN and ANFIS and the mechanistic modelling in eriochrome black-T dye adsorption using modified clay. South African Journal of Chemical Engineering, 2021;36:24-42. Available: <https://doi.org/10.1016/j.sajce.2020.12.003>

© 2022 Nwobasi et al.; This is an Open Access article distributed under the terms of the Creative Commons Attribution License (<http://creativecommons.org/licenses/by/4.0>), which permits unrestricted use, distribution, and reproduction in any medium, provided the original work is properly cited.

*Peer-review history:*

*The peer review history for this paper can be accessed here:*

*<https://www.sdiarticle5.com/review-history/87836>*